2024 IEEE International Conference on Robotics and Automation (ICRA 2024)
May 13-17, 2024. Yokohama, Japan

Human-Robot Complementary Collaboration for Flexible and Precision Assembly

Shichen Cao[1] and Jing Xiao[1]

***Abstract*— This paper addresses human-robot collaborative (HRC) precision assembly that complements natural human ability and the strength of an autonomous robot system. Our approach enables both flexibility and efficiency of tight-clearance assembly of various complex-shaped parts in the presence of uncertainty without requiring assembly skills and knowledge of robotics from the human operator. We demonstrated the effectiveness of our approach in a variety of experiments and comparisons with other HRC assembly approaches.**

***Index Terms*— Human-robot collaboration, compliant assembly, human-centered automation.**

I. Introduction

It is challenging to achieve both flexibility and efficiency in tight-clearance assembly. Traditional manual assembly requires extensive training for workers and often results in quality variations and productivity fluctuations. Additionally, such tasks can pose health and safety risks to human workers [1]. The advance of robotics research has led to significant development in automating repetitive assembly tasks in controlled environments, achieving high efficiency [2]. However, existing robotic assembly systems are often designed for specific tasks, limited in perception, and lack the flexibility to perform a variety of assembly tasks. To bridge this gap, HRC systems are promising to offer a solution by combining human adaptability and robot precision [3].

Earlier work on HRC systems often uses the robot as a tool performing specific, independent sub-tasks without direct human interaction. Such robots typically handle tasks like picking, placing, transporting and holding [4], [5], [6], either following a pre-defined path [7] or being guided by human operators using via teleoperation [8]. In recent years, more studies started to explore the robot as a partner to provide necessary assistance intelligently, taking advantage of vision perception coupled with learning-based algorithms [9], [10], [11], [12], [13]. Robots can perform human-aware autonomous tasks [14], plan motion [15], and perform task planning and allocation [16] based on human motion predictions or gesture recognition [17], [18]. A recent study [19] proposes a collaborative robot system that tracks high-level intentions to estimate human interaction patterns and avoid collisions, while low-level intentions provide task-related information to the robot. However, the assistance provided by the robot is very limited and can only facilitate simple assembly operations designed for specific tasks. The robot assistance relies heavily on the human operators' ability since the human workers do the final assembly.

HRC systems in assembly tasks currently fall short of effectively leveraging the complementary capabilities of human workers and autonomous robots for precise, flexible, and efficient assembly.

This paper introduces a novel approach for human-robot collaboration in assembly, which enables the human operator to provide simple guidance of gross robot motion while the robot handles the actual, complex assembly process, taking full advantage of the natural capabilities of humans and the strengths of an autonomous robotic assembly algorithm [20]. Specifically, it makes the following contributions:

- Workspace Mapping: translates low-precision human actions into high-precision robotic movements.
- Human-Robot Synchronization: aligns human gestures at the same time with robot movement.
- Seamless Motion Transition: shifts from human-guided to autonomous robot motions quickly, requiring minimal training.
- Guided Autonomy: uses simple human guidance to enable autonomous robotic batch assembly of complex parts in arbitrary locations.

The effectiveness of the approach is demonstrated through a case study focusing on complex and precise insertion tasks.

The subsequent sections of the paper are structured as follows: Section II describes our HRC system and elaborates on enabling autonomous robotic batch assembly. Section III presents experimental results and a comparative analysis. Section IV concludes the paper.

II. HRC Assembly System

Our system features a general-purpose robot manipulator equipped with a force/torque sensor and the HTC VIVE controller [21] as the human interaction device given its advantages on 6-DOF tracking, portability, minimal hardware needs, and unrestricted movement. The HTC VIVE device is intuitive to use and requires minimal training of the human operator. The system supports interchangeable robotic grippers on the manipulator to meet different picking needs. Our HRC assembly system enables the human operator to guide the robot manipulator to pick up a part and transfer it to the desired assembly area for an autonomous system to take over and perform the assembly.

[1]Shichen Cao and Jing Xiao are with the Robotics Engineering Department, Worcester Polytechnic Institute, Worcester, MA 01609, USA. Email: scao3@wpi.edu; jxiao2@wpi.edu

The work was supported by funding from the US Army DEVCOM Analysis Center under Cooperative Agreement Number W911NF-22-2-0001.

A. Workspace Mapping

Establishing an effective mapping relationship between the operator's movements and the robot's workspace is pivotal for two main reasons: to ensure that the robot's range of motion is not limited by the operator's arm span and the operator's coarse motion resolution and to maintain safety. We introduce a dynamic sub-workspace remapping approach to convert low-precision human actions into high-precision robotic movements.

We define the human operator's workspace as a rectangular bounding box A, and A also denotes its coordinate system with the origin at the centroid and axes aligned with the edges of the rectangular box. Initially, the operator holds the VIVE controller with the right hand (or the left hand), and extends the corresponding arm towards the eight reachable extremities, as depicted in Fig. 1, where the operator's rectangular workspace is decided by using the right hand to reach and record the extreme positions. Note that the extreme points are not necessarily the same as the vertices of the rectangular workspace, which is the maximum cuboid within the region bounded by the collected extreme points.

We define a rectangular region within the robot manipulator's workspace as B, which also indicates its coordinate system with the origin at the centroid of the cuboid and axes aligned with the edges of the cuboid. The region B can be established by the operator via moving the robot arm to make sure that it is within the dexterous workspace of the robot.

Let the position of each vertex of region A be $\mathbf{v}_{A_i}$, where $i = 1, \ldots, 8$. The vertex corresponding to $\mathbf{v}_{A_i}$ in region B of the robot's workspace is denoted as $\mathbf{v}_{B_i}$. We adopt the Procrustes analysis [22] to discern the optimal transformation between regions A and B and employ singular value decomposition (SVD) [23] to derive the rotation matrix. For the sake of brevity, we use X to denote either A or B. Let $\mathbf{d}_{X_i}$ represent the distance of each i^{th} point to the workspace's centroid:

$$\mathbf{d}_{X_i} = \mathbf{v}_{X_i} - \frac{1}{8}\sum_{i=1}^{8}\mathbf{v}_{X_i}. \tag{1}$$

The scaling factor α can be derived as:

$$\alpha = \sqrt{\frac{\sum_{i=1}^{8}\mathbf{d}_{B_i}^T \cdot \mathbf{d}_{B_i}}{\sum_{i=1}^{8}\mathbf{d}_{A_i}^T \cdot \mathbf{d}_{A_i}}}. \tag{2}$$

We then apply SVD to compute the rotation matrix R, which represents the transformation from coordinate system A to coordinate system B:

$$U \cdot \Sigma \cdot V^T = \sum_{i=1}^{8}\alpha\mathbf{d}_{A_i} \cdot \mathbf{d}_{B_i}^T, R = V^T \cdot U^T, \tag{3}$$

where U and V are orthogonal matrices, and Σ is a diagonal matrix with singular values. Hence, for any point $\mathbf{p}_{A_j}$ of the region A, the corresponding mapped point of the region B satisfies:

$$\mathbf{p}_{B_j} = \alpha R \cdot (\mathbf{p}_{A_j} - \frac{1}{8}\sum_{i=1}^{8}\mathbf{v}_{A_i}) + \frac{1}{8}\sum_{i=1}^{8}\mathbf{v}_{B_i}. \tag{4}$$

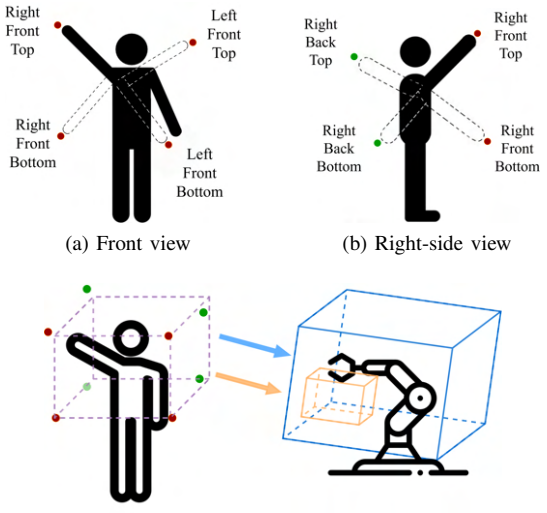

(a) Front view (b) Right-side view

(c) Workspace mapping

Fig. 1. Determining and mapping human operator's workspace to robot's workspace. Red points: extremities in the front. Green points: extremities at the back. Purple box: region A. Blue box: region B. Yellow box: robot's sub-workspace.

Furthermore, we introduce a dynamic sub-workspace remapping function that adaptively recalibrates the operator's physical range of motion to correspond to a selected subregion of B for fine manipulation. This is particularly useful for guiding fine robot motions that involve contacts of the held part and another part. Re-mapping the human operator's workspace to a smaller region of the robot's workspace, or sub-workspace, can prevent slight gestures by the operator resulting in large movements of the robot's arm and end-effector. Sub-workspace remapping is achieved by reducing the scaling factor to a smaller value, denoted as α', and setting a centroid offset, $\mathbf{\Delta} = [\Delta x, \Delta y, \Delta z]^T$. Thus, (4) is modified as:

$$\mathbf{p}_{B_j} = \alpha' R \cdot (\mathbf{p}_{A_j} - \frac{1}{8}\sum_{i=1}^{8}\mathbf{v}_{A_i}) + \frac{1}{8}\sum_{i=1}^{8}\mathbf{v}_{B_i} + \mathbf{\Delta}. \tag{5}$$

The sub-workspace mapping can be dynamically adjusted as needed to accommodate changes in the workspace or the operator's position. This approach ensures that the end-effector can safely maneuver to any desired pose within the robot's workspace, making it convenient for human operators without any prior training. By limiting the robot's operations to a more focused region, our system effectively transforms broader, low-precision human gestures into intricate, high-precision robot end-effector movements, which is essential for tasks that require a delicate touch or fine-tuned motion.

B. Human-Robot Motion Synchronization

The primary objective of human-robot motion synchronization is to (i) determine inverse kinematics (IK) solutions swiftly for the human operator's gesture, (ii) ensure low-latency data communication, and (iii) enable rapid trajectory planning for the robot to navigate to the corresponding target pose [24], [25].

(i) Swift IK solution: We utilize a sequential quadratic programming (SQP) method [26], which employs quasi-Newton techniques for optimal joint limit handling, to solve IK for each target pose. Upon data acquisition from the controller, the position $\mathbf{p}_{A_j}$ and orientation $\mathbf{r}_{A_j} = [\phi, \theta, \psi]^T$ are retrieved using OpenVR API [27]. Using (4), we deduce the robot's mapped position $\mathbf{p}_{B_j}$ from $\mathbf{p}_{A_j}$, and the mapped orientation follows $\mathbf{r}_{B_j} = \mathbf{r}_{A_j}$. As a result, we formulate the 6-D target pose $\mathbf{P}_B$ in the robot's workspace as $[x, y, z, \phi, \theta, \psi]^T$. By resolving the SQP in joint space instead, we ensure each solution occurs within $1ms$.

(ii) Low-latency communication: Synchronization between the robot's movements and human intentions requires low latency, which is crucial for seamless interaction and safety. We adopted a decentralized control architecture, as shown in Fig. 2, to achieve minimal data communication latency between multiple devices. A client computer is connected to the HTC devices to obtain and extract real-time positional data and button signals while a real-time kernel server is equipped to receive the data for communication with the robot arm. This data is time-stamped to synchronize the devices using the Robot Operating System (ROS). Such a decentralized control system helps distribute the computation load and reduces the overall system latency.

(iii) Rapid trajectory planning: The necessity for swift trajectory planning arises from its essential role in ensuring safety and immediacy in response to human actions, while enhancing efficiency in task performance. We employ the MoveIt framework [28] to generate the trajectory towards the target pose. Furthermore, we adopt the autoregressive integrated moving average (ARIMA) approach [29] to use historical pose data added with timestamps to predict upcoming reference poses. The IK for these anticipated poses is pre-solved to produce a reference trajectory set. Once an incoming $\mathbf{P}_B$ matches a reference pose, the robot can bypass the IK and planning processes and directly execute the pre-compiled trajectory from the reference set. The real-time feedback constantly tracks the end-effector's pose and ensures prompt pose switches.

In addition, we designed a stabilization system combining simple moving average [30] and a Schmitt trigger. This system inhibits minor movements of the robot's end-effector, triggered by involuntary human hand tremors when the operator tries to keep the controller steady [31]. Without the system, rapid data transmission would render the robot's pose extremely responsive to even minuscule operator movements.

C. Effortless Control of Human-Guided Motions and Shift to Autonomous Robot Motions

To facilitate the operator's efficient guidance of the robot manipulator, we utilize the buttons on the controller, as depicted in Fig. 2. By programming the button signals with the bit-shifting method, we implement functionalities that optimize the robot's movements in the presence of inaccuracies in operator actions, as detailed in the following.

Menu button: allows for an immediate reset of the robot to its predefined home pose. This is particularly useful in situations where the robot arm becomes jammed.

Trackpad: enables rapid speed and acceleration for long robot translation and provides controlled deceleration for fine manipulations. Also, when the end-effector's orientation closely aligns with the desired pose, further rotation becomes redundant, as only translation is needed. In such a case, the trackpad both modulates the robot's speed and immobilizes the end-effector's rotation (roll, pitch, and yaw).

Grip button: initiates a grasping action using any compatible gripper, such as a two-finger or a vacuum gripper.

Trigger: activate the autonomous assembly algorithm once the end-effector is positioned near the desired pose.

For tasks that require flexible assembly of varied parts, our system capitalizes on innate human abilities, and allows the user to easily perceive, select components, and direct the robot to the target assembly area. The system ensures a seamless transition from human-guided movements, to autonomous robotic motion to perform the actual assembly.

D. Autonomous Robotic Batch Assembly from Human Guidance

As previously introduced, current studies in the HRC system for assembly tasks place a significant burden on human operators. Typically, high-complexity assembly tasks are delegated to humans while robots are relegated to low-complexity supporting tasks (such as providing a part).

Our approach employs the robot to conduct the actual assembly of complex parts using a general, autonomous robotic assembly approach [20] while letting the human operator simply direct the robot to the parts for assembly. The autonomous robotic assembly approach is general to parts of all shapes and can handle large uncertainties 10 times of the task tolerance via force/torque sensing efficiently. By integrating this approach, we achieve autonomous robotic batch assembly for varied and complex-shaped parts with human guidance.

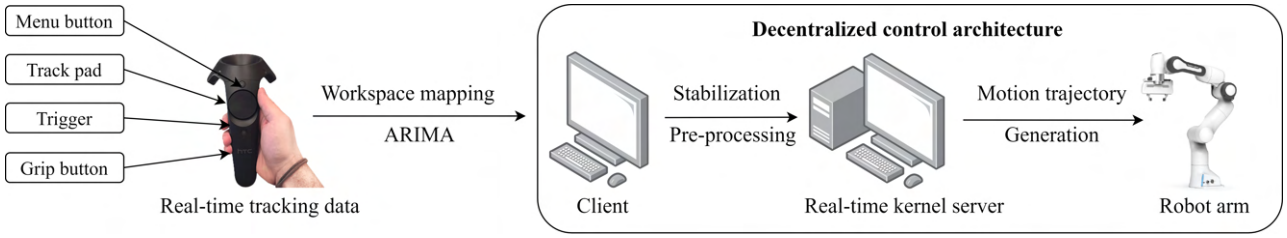

Fig. 2. Human-robot motion synchronization in the HRC assembly system.

Consider two batches of complex-shaped parts for assembly: the male and female parts batch, denoted as M and F, respectively. Individual parts within these batches are represented by M_i and F_j, where i, j are their indices, respectively. The parts within the same batch can be different.

Initially, the human operator uses the interaction device to move the robot to M and presses the grip button to pick up a chosen part, M_i. Next, the operator directs the robot, which is now holding the part, toward the assembly site. Once M_i is close to the desired female part, F_j, the trigger button can be pressed to activate the autonomous assembly algorithm that takes over the assembly process. The human operator's guidance does not have to be precise. In other words, there can be both position and orientation uncertainties between the gripper and M_i, as well as between the held M_i and F_j. The algorithm can estimate and overcome the uncertainties to accomplish the assembly task. To further ensure efficiency and robustness, the robot operates at high speeds during human-guided gross motions, and adopts a slower pace as the held M_i is close to F_j for contact-rich automatic assembly.

After the human operator guides the robot to a particular part and its goal part for assembly once, the autonomous system can take over the entire process of part picking, transferring, and assembling at (roughly) the same locations for the same parts if provided. This enables a batch operation of the same assembly task. Moreover, if the human operator guides the robot to fetch different parts at different locations and to different assembly destinations once, the autonomous system can take over next to conduct a batch operation of different kinds of assembly tasks flexibly.

Such batch operations can free up the human operator to conduct other tasks. If there are multiple small batches of different parts for assembly, our HRC assembly approach not only enables a single robot to perform different assemblies flexibly but also allows a single human operator to assist multiple robots to achieve different assemblies simultaneously to increase productivity. Additionally, for tasks involving the assembly of multiple parts, the human operator can guide the robot to perform the assembly steps once, and then the autonomous system can take over to conduct the entire sequence of assembly autonomously.

III. Experiments of Assembly with Multi-Peg-in-Hole Structures

We implemented our assembly system using a Franka Panda arm [32], equipped with an ATI force/torque sensor [33] and a Schmalz vacuum gripper [34], as illustrated in Fig. 3a. The pickup zones, $\mathbf{P_1}$ and $\mathbf{P_2}$, as well as the assembly zones $\mathbf{A_1}$-$\mathbf{A_3}$, are exemplified as they can be anywhere within the robot's workspace. Fig. 3b-3e displays multi-peg parts randomly placed in the pickup zones. $\mathbf{Obj_1}$, $\mathbf{Obj_2}$, and $\mathbf{Obj_3}$, were designed with varying angles between the suction surface and a multi-peg prism: $0°$ (parallel), $20°$, and $25°$ respectively, for experiments with different insertion directions. The hole structures are securely fixed using connectors oriented at $30°$, $0°$, and $45°$ angles relative to the workbench within the assembly zones to increase the assembly challenge. The clearance in orientation and position between a multi-peg structure and the corresponding multi-hole structure is less than $0.015rad$ and $1.5mm$ respectively.

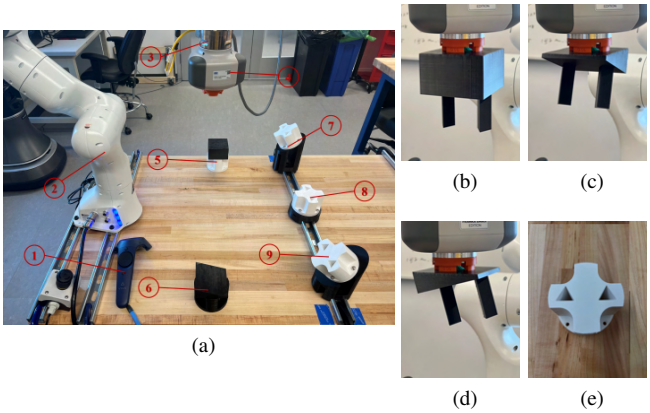

(a) (b) (c) (d) (e)

Fig. 3. (a) The environment setup for experiments: (1) VIVE controller, (2) robot, (3) force/torque sensor, (4) vacuum gripper, (5)-(6) pickup zones $\mathbf{P_1}$ and $\mathbf{P_2}$, (7)-(9) assembly zones $\mathbf{A_1}$-$\mathbf{A_3}$. (b) $\mathbf{Obj_1}$. (c) $\mathbf{Obj_2}$. (d) $\mathbf{Obj_3}$. (e) Hole Structure.

In each trial, the human operator uses the VIVE controller to guide the robot in picking up and transferring various parts to different assembly zones, which are unknown to the system beforehand. During the pickup phase, the suction cup might come into contact with any part of the multi-peg structure, adding another source of pose uncertainty. Once the vacuum gripper secures the multi-peg part, the human operator can select a desired assembly zone. The robot's joint speed is set at $2rad/s$ during human-guided gross motion, and $0.5rad/s$ prior to any contact motion in the assembly.

A. Human-Guided Multi-Peg-in-Hole Assemblies

In Fig. 4, we present an example of an assembly utilizing our HRC assembly approach. Initially, the human operator used the controller to direct the robot towards a part in the pickup zone $\mathbf{P_2}$ (Fig. 4a). Next, the operator activated the grip button to allow the vacuum gripper to lift the part $\mathbf{Obj_2}$ (Fig. 4b). The operator then guided the robot held the part to the assembly zone, $\mathbf{A_2}$ in this case (Fig. 4c). Once the peg structure was roughly aligned with the hole structure, the operator activated the algorithm for autonomous assembly (Fig. 4d). As the held part made contact with the hole structure, the relative uncertainty and contact configuration were estimated based on force/torque measurements (Fig. 4e). Using this estimation, a recovery motion was generated to move the part to its updated relative goal pose. To prevent collisions and to realign the insertion direction, the robot slightly retracted the held part from the contact along its original path before the insertion (Fig. 4f). Upon successful insertion, the gripper was deactivated to release the part, and the robot returned to the home configuration. The robot's poses at both the pickup and assembly zones were logged to facilitate subsequent batch assembly if needed.

To evaluate the performance of our HRC assembly system, we conducted 110 assembly task experiments with varying

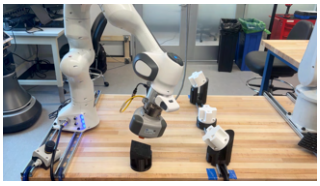

(a) Human operator guides the robot to pickup zone.

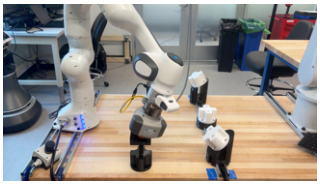

(b) Vacuum gripper is activated to pick up and pull out the part.

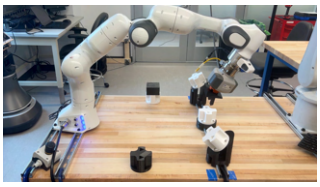

(c) Human operator guides the robot to the assembly zone.

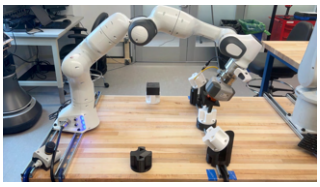

(d) Autonomous assembly algorithm is activated.

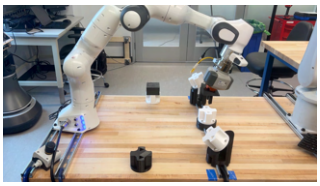

(e) Estimate the uncertainty and correct the insertion direction.

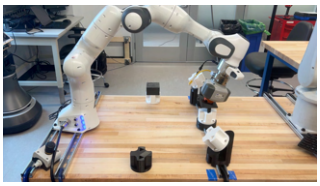

(f) Assembly is accomplished.

Fig. 4. Human operator-guided autonomous assembly task.

pickup zones, assembly zones, and insertion angles. Our system achieved an overall success rate of 97%. Table I details the performance for 8 of these cases. The "uncertainties" column depict the 6-dimensional relative orientations and the positional pose differences between the peg and hole structures, as predicted by the algorithm. As shown, the orientation uncertainty exceeds **10** times of the task clearance ($0.015rad$), and the position uncertainty is approximately **4** times of the task clearance ($1.5mm$). Notably, the positions of pickup zones $\mathbf{P_1}$ and $\mathbf{P_2}$ varied across cases, as they were placed randomly on the workbench. The robot mimicked human movement in real time, and it took less than 20 seconds to do so in our experiments. The autonomous assembly process took about 5 seconds in each case. The average overall motion execution time was about 32 seconds.

Despite a generally high success rate, we had 3 failures (out of 110 tests) during human-guidance assembly in zones $\mathbf{A_1}$ and $\mathbf{A_3}$. The primary cause was that the human-guided operation led to a level of relative uncertainties between parts that exceeded the automatic algorithm's allowed bounds. Such situation is difficult to detect sometimes by the human operator before the autonomous assembly operation starts. One simple solution to solve the problem is to increase the allowed uncertainty bounds of the autonomous system.

B. Automatic Multi-Peg-in-Hole Assemblies

Once a human operator has guided the robot through an assembly process, the robot can autonomously conduct the process by picking up a part from the same pickup location and assembling it at the same assembly location. The performance for autonomous assembly tasks is detailed in Table II. The experiments involved various pickup and assembly zones as well as insertion angles. Specifically:

- Cases 1-4 show the performance of batch operation of (20) individual assembly tasks in each case.
- Cases 5 and 6 show the performance of batch operation of (5) combined assembly tasks in each case.

Overall, a success rate of 96.7% was achieved. Note that the object pose information at pickup and assembly zones was subject to inaccuracy and uncertainty, but the autonomous assembly algorithm overcame the uncertainties as expected. Compared to human-guided assembly, the automatic individual assembly process took only about half of the execution time with the same high success rate.

For combined assembly tasks, the total time, including the transition time between different sub-tasks, was almost the same as the sum of the times taken for each individual assembly task, regardless of object shapes and assembly locations. This shows the efficiency of our system to handle a sequence of assembly operations. In case additional components are required for one specific task, the human operator has the flexibility to redirect the robot to obtain the required part from a different pickup location.

TABLE I. THE PERFORMANCE OF HUMAN-ROBOT COLLABORATION SYSTEM IN MIX-SHAPED MULTI-PEG-IN-HOLE ASSEMBLY TASKS

Case	Pickup Zone	Assembly Zone	Insertion Angle	Motion Execution Time (s)				Uncertainties		Result
				Picking	Placing	Autonomous	Total	Orientation (*rad*)	Position (*mm*)	
1	$\mathbf{P_1}$	$\mathbf{A_1}$	$\mathbf{Obj_1}$ - 0°	8.2	13.0	5.4	26.6	$[-0.15, -0.12, -0.18]$	$[-2.3, 3.0, 0.3]$	✓
2	$\mathbf{P_1}$	$\mathbf{A_1}$	$\mathbf{Obj_2}$ - 20°	13.2	16.6	3.7	33.5	$[0.19, -0.12, -0.02]$	$[-2.9, -4.6, 0.1]$	✓
3	$\mathbf{P_1}$	$\mathbf{A_1}$	$\mathbf{Obj_3}$ - 25°	15.6	14.8	4.1	34.5	$[-0.10, -0.18, -0.18]$	$[-3.8, 2.0, 0.5]$	✓
4	$\mathbf{P_1}$	$\mathbf{A_2}$	$\mathbf{Obj_1}$ - 0°	9.5	12.6	5.0	27.1	$[-0.19, 0.04, -0.01]$	$[0.9, 4.5, -0.7]$	✓
5	$\mathbf{P_2}$	$\mathbf{A_2}$	$\mathbf{Obj_3}$ - 25°	18.8	19.4	4.6	42.8	$[0.08, -0.15, 0.14]$	$[-3.3, -1.5, 0.5]$	✓
6	$\mathbf{P_2}$	$\mathbf{A_3}$	$\mathbf{Obj_1}$ - 0°	8.5	12.5	4.0	25.0	$[0.17, 0.11, 0.13]$	$[2.6, -2.8, -1.0]$	✓
7	$\mathbf{P_2}$	$\mathbf{A_3}$	$\mathbf{Obj_2}$ - 20°	16.5	13.4	3.8	33.7	$[-0.15, -0.09, 0.03]$	$[-2.3, 3.7, 0.2]$	✓
8	$\mathbf{P_2}$	$\mathbf{A_3}$	$\mathbf{Obj_3}$ - 25°	17.9	15.0	4.9	37.8	$[0.19, 0.12, -0.07]$	$[2.2, -5.0, -1.3]$	✓

TABLE III. THE COMPARISON WITH RECENT HRC SYSTEMS

Method	Robot Operation	Human Operation	Assembly Task	Time (seconds)	Object Shape Complexity	Task Flexibility
[19]	Estimate human's intention to assist human motion	Object transferring, preparation and assembly	Object Push-In	≈ 25	Multi-round	Yes
[35]	Body gestures recognition and object transfer	Gestures command Object placement	Peg-in-Hole	≈ 70	Single round	Yes
[36]	Hand gestures and voice recognition	Gesture/voice command assembly	Engine Part Insertion	≈ 100	Dual round	No
[37]	Force/vision sensing to assist human motion	Object transferring assembly	Peg-in-Hole	≈ 20	Single round	No
Ours	Object picking, transferring, and autonomous assembly	Intuitive guidance	Peg-in-Hole	< 20	Complex multi-peg	Yes

TABLE II. THE PERFORMANCE OF AUTOMATIC BATCH ASSEMBLY OPERATIONS OF MIX-SHAPED, MULTI-PEG-IN-HOLE TASKS

Case	Pickup Zone	Assembly Zone	Insertion Angle	Success / Runs	Average Time (s)
1	$\mathbf{P_1}$	$\mathbf{A_1}$	$\mathbf{Obj_1}$ - 0°	20 / 20	16.0
2	$\mathbf{P_2}$	$\mathbf{A_2}$	$\mathbf{Obj_2}$ - 20°	20 / 20	15.8
3	$\mathbf{P_1}$	$\mathbf{A_1}$	$\mathbf{Obj_3}$ - 25°	19 / 20	17.4
4	$\mathbf{P_2}$	$\mathbf{A_3}$	$\mathbf{Obj_2}$ - 20°	18 / 20	17.2
5	$\mathbf{P_1}$	$\mathbf{A_1}$	$\mathbf{Obj_1}$ - 0°	5 / 5	38.5
	$\mathbf{P_2}$	$\mathbf{A_2}$	$\mathbf{Obj_2}$ - 20°		
6	$\mathbf{P_2}$	$\mathbf{A_1}$	$\mathbf{Obj_1}$ - 0°	5 / 5	50.2
	$\mathbf{P_1}$	$\mathbf{A_2}$	$\mathbf{Obj_2}$ - 20°		
	$\mathbf{P_2}$	$\mathbf{A_3}$	$\mathbf{Obj_3}$ - 20°		

A contributing factor to the failures in some of the automatic assembly experiments (about 3% of all cases) is the immediate dissipation of force/torque after contact, as the vacuum gripper could not maintain a stable force/torque by continually pushing the end-effector towards the peg object. One effective solution is to use an active compliant control strategy to allow the robot gripper to react promptly to the contact force/torque and adjust its movements to maintain stable force through the assembly process. Thus, the system can obtain more precise and consistent force/torque data.

C. Comparative Study

Table III contrasts our method with recent HRC work for assembly tasks. As shown in the table, these existing studies put the burden of perception to the robot systems to detect the human operator's needs via sensing, such as force, vision, gesture, and voice recognition, while the human operator does the actual assembly manually and only for round-shaped objects. Such approaches do not take full advantage of the complementary strengths of natural human perception and robotic efficiency and consistency. The final column, labeled "Task Flexibility," indicates whether the method can be applicable to various assembly tasks (rather than specifically crafted for a particular task). Note that only one experiment was conducted once in [35], [36] respectively, and [37] reported running one experiment three times successfully. In contrast, our approach achieved a remarkable success rate of 27 out of 30 runs of a variety of assembly tasks. It provides a highly flexible and operator-friendly solution for a wide range of assembly operations to allow easy reconfiguration of the work environment for different assemblies and ensure high efficiency and a high success rate.

The attached video shows example executions of the system for assembly tasks with different objects, pickup zones, and assembly zones.

IV. CONCLUSIONS

We introduced a novel system for human-robot collaboration in conducting assembly tasks. This system leverages the innate ability of a human operator combined with the robustness and efficiency of an autonomous robotic assembly system to achieve high flexibility and efficiency. The introduced system aims to minimize the need to train human workers and to spare them from conducting boring, non-ergonomic, or strenuous operations to increase their job quality. Our experiments have shown success of the system in effectively tackling challenging assembly tasks of tight-clearance and involving complex-shaped parts, under the guidance of a human operator with minimum training. Once the operator guided the robot to complete an assembly task or a sequence of assembly tasks, the robot can automatically perform the same task or sequence of tasks in batch operation, thereby freeing the human operator to work on other tasks.

Our future research will involve a user study to let individuals with diverse backgrounds and no prior experience in robotics operate our human-robot complementary collaboration system for assembly. The study aims to further validate the user friendliness, robustness, and efficiency of the system. We also plan to further extend and improve the basic system to allow concurrent operations of a human operator and one or more general-purpose robot manipulators to maximize both flexibility and productivity for high-precision, small-patch assembly tasks that frequently change or complex assembly tasks that include those requiring dual-arm operations.

REFERENCES

[1] N. Edmondson and A. Redford, "Generic flexible assembly system design," *Assembly automation*, vol. 22, no. 2, pp. 139–152, 2002.

[2] Y.-C. Chiang, H. Bier, and S. Mostafavi, "Design to robotic assembly: An exploration in stacking," *Frontiers in Digital Humanities*, vol. 5, p. 23, 2018.

[3] E. Matheson, R. Minto, E. G. Zampieri, M. Faccio, and G. Rosati, "Human–robot collaboration in manufacturing applications: A review," *Robotics*, vol. 8, no. 4, p. 100, 2019.

[4] G. Michalos, N. Kousi, P. Karagiannis, C. Gkournelos, K. Dimoulas, S. Koukas, K. Mparis, A. Papavasileiou, and S. Makris, "Seamless human robot collaborative assembly–an automotive case study," *Mechatronics*, vol. 55, pp. 194–211, 2018.

[5] V. Gopinath, F. Ore, S. Grahn, and K. Johansen, "Safety-focussed design of collaborative assembly station with large industrial robots," *Procedia manufacturing*, vol. 25, pp. 503–510, 2018.

[6] J. T. C. Tan, Y. Zhang, F. Duan, K. Watanabe, R. Kato, and T. Arai, "Human factors studies in information support development for human-robot collaborative cellular manufacturing system," in *RO-MAN 2009 - The 18th IEEE International Symposium on Robot and Human Interactive Communication*, 2009, pp. 334–339.

[7] U. Othman and E. Yang, "Human–robot collaborations in smart manufacturing environments: review and outlook," *Sensors*, vol. 23, no. 12, p. 5663, 2023.

[8] S. Lichiardopol, "A survey on teleoperation," *Technische Universitat Eindhoven, DCT report*, vol. 20, pp. 40–60, 2007.

[9] I. D. Walker, L. Mears, R. S. Mizanoor, R. Pak, S. Remy, and Y. Wang, "Robot-human handovers based on trust," in *2015 Second International Conference on Mathematics and Computers in Sciences and in Industry (MCSI)*. IEEE, 2015, pp. 119–124.

[10] B. Sadrfaridpour and Y. Wang, "Collaborative assembly in hybrid manufacturing cells: An integrated framework for human–robot interaction," *IEEE Transactions on Automation Science and Engineering*, vol. 15, no. 3, pp. 1178–1192, 2017.

[11] H. Liu, T. Fang, T. Zhou, Y. Wang, and L. Wang, "Deep learning-based multimodal control interface for human-robot collaboration," *Procedia CIRP*, vol. 72, pp. 3–8, 2018.

[12] Q. Liu, Z. Liu, B. Xiong, W. Xu, and Y. Liu, "Deep reinforcement learning-based safe interaction for industrial human-robot collaboration using intrinsic reward function," *Advanced Engineering Informatics*, vol. 49, p. 101360, 2021.

[13] Z. Jin, A. Liu, W.-A. Zhang, L. Yu, and C.-Y. Su, "A learning based hierarchical control framework for human–robot collaboration," *IEEE Transactions on Automation Science and Engineering*, vol. 20, no. 1, pp. 506–517, 2023.

[14] A. M. Zanchettin, A. Casalino, L. Piroddi, and P. Rocco, "Prediction of human activity patterns for human–robot collaborative assembly tasks," *IEEE Transactions on Industrial Informatics*, vol. 15, no. 7, pp. 3934–3942, 2018.

[15] V. V. Unhelkar, P. A. Lasota, Q. Tyroller, R.-D. Buhai, L. Marceau, B. Deml, and J. A. Shah, "Human-aware robotic assistant for collaborative assembly: Integrating human motion prediction with planning in time," *IEEE Robotics and Automation Letters*, vol. 3, no. 3, pp. 2394–2401, 2018.

[16] K. Darvish, B. Bruno, E. Simetti, F. Mastrogiovanni, and G. Casalino, "Interleaved online task planning, simulation, task allocation and motion control for flexible human-robot cooperation," in *2018 27th IEEE International Symposium on Robot and Human Interactive Communication (RO-MAN)*, 2018, pp. 58–65.

[17] T. Ende, S. Haddadin, S. Parusel, T. Wüsthoff, M. Hassenzahl, and A. Albu-Schäffer, "A human-centered approach to robot gesture based communication within collaborative working processes," in *2011 IEEE/RSJ International Conference on Intelligent Robots and Systems*, 2011, pp. 3367–3374.

[18] W. Wang, R. Li, Z. M. Diekel, Y. Chen, Z. Zhang, and Y. Jia, "Controlling object hand-over in human–robot collaboration via natural wearable sensing," *IEEE Transactions on Human-Machine Systems*, vol. 49, no. 1, pp. 59–71, 2018.

[19] Z. Huang, Y.-J. Mun, X. Li, Y. Xie, N. Zhong, W. Liang, J. Geng, T. Chen, and K. Driggs-Campbell, "Hierarchical intention tracking for robust human-robot collaboration in industrial assembly tasks," in *2023 IEEE International Conference on Robotics and Automation (ICRA)*. IEEE, 2023, pp. 9821–9828.

[20] S. Cao and J. Xiao, "A general method for autonomous assembly of arbitrary parts in the presence of uncertainty," in *2022 IEEE/RSJ International Conference on Intelligent Robots and Systems (IROS)*, 2022, pp. 10 259–10 266.

[21] H. Corporation, "HTC Vive," 2016, virtual Reality Headset. [Online]. Available: https://www.vive.com/

[22] A. Ross, "Procrustes analysis," *Course report, Department of Computer Science and Engineering, University of South Carolina*, vol. 26, pp. 1–8, 2004.

[23] E. Henry and J. Hofrichter, "[8] singular value decomposition: Application to analysis of experimental data," in *Methods in enzymology*. Elsevier, 1992, vol. 210, pp. 129–192.

[24] Y. Li and S. S. Ge, "Force tracking control for motion synchronization in human-robot collaboration," *Robotica*, vol. 34, no. 6, pp. 1260–1281, 2016.

[25] W. Xu, X. Li, W. Xu, L. Gong, Y. Huang, Z. Zhao, L. Zhao, B. Chen, H. Yang, L. Cao *et al.*, "Human-robot interaction oriented human-in-the-loop real-time motion imitation on a humanoid tri-co robot," in *2018 3rd International Conference on Advanced Robotics and Mechatronics (ICARM)*. IEEE, 2018, pp. 781–786.

[26] P. Beeson and B. Ames, "Trac-ik: An open-source library for improved solving of generic inverse kinematics," in *2015 IEEE-RAS 15th International Conference on Humanoid Robots (Humanoids)*. IEEE, 2015, pp. 928–935.

[27] S. OpenVR, "Openvr sdk," *ValveSoftware/openvr*.

[28] D. Coleman, I. Sucan, S. Chitta, and N. Correll, "Reducing the barrier to entry of complex robotic software: a moveit! case study," *arXiv preprint arXiv:1404.3785*, 2014.

[29] R. H. Shumway, D. S. Stoffer, R. H. Shumway, and D. S. Stoffer, "Arima models," *Time series analysis and its applications: with R examples*, pp. 75–163, 2017.

[30] R. J. Hyndman, "Moving averages." 2011.

[31] T. Tsumugiwa, R. Yokogawa, and K. Hara, "Variable impedance control with virtual stiffness for human-robot cooperative peg-in-hole task," in *IEEE/RSJ International Conference on Intelligent Robots and Systems*, vol. 2, 2002, pp. 1075–1081 vol.2.

[32] F. E. GmbH. Franka control interface documentation. [Online]. Available: https://frankaemika.github.io/docs/

[33] ATI. ATI Industrial Automation: F/T Sensor Gamma. [Online]. Available: https://www.ati-ia.com/products/ft/ft_models.aspx?id=gamma

[34] Schmalz. Schmalz Cobot Pump Franka Emika Edition. [Online]. Available: https://www.franka.de/ecosystem

[35] P. Tsarouchi, A.-S. Matthaiakis, S. Makris, and G. Chryssolouris, "On a human-robot collaboration in an assembly cell," *International Journal of Computer Integrated Manufacturing*, vol. 30, no. 6, pp. 580–589, 2017.

[36] S. Liu, L. Wang, and X. V. Wang, "Function block-based multimodal control for symbiotic human–robot collaborative assembly," *Journal of Manufacturing Science and Engineering*, vol. 143, no. 9, 2021.

[37] Y. Yamakawa, Y. Matsui, and M. Ishikawa, "Development of a real-time human-robot collaborative system based on 1 khz visual feedback control and its application to a peg-in-hole task," *Sensors*, vol. 21, no. 2, p. 663, 2021.